

An Optimized iFEM for High Precision Real-Time Deformation Sensing of Composite Antenna Panel

WENPENG DUAN, SHENFANG YUAN* and JIAN CHEN

ABSTRACT

In recent years, composite structures have gained extensive applications in the aerospace industry owing to their high strength-to-weight ratio, lightweight nature, and superior corrosion resistance. Notable examples include large phased-array antenna panels, composite wing skins, wing box sections, fuel tanks, and rocket fairings, etc. Taking the large phased-array antennas as a representative case, their antenna panels are constructed from multi-layered heterogeneous honeycomb sandwich panel, and serve as critical components for hosting functional elements of satellite antennas, which play a pivotal role in enabling core satellite functionalities. However, during on-orbit operations, these panels are exposed to the harsh and complex space environment, inevitably leading to unpredictable structural deformations that jeopardize satellite performance and operational safety. Consequently, research on deformation sensing for composite antenna panels holds significant engineering urgency. Among various deformation sensing methodologies, the inverse Finite Element Method (iFEM) has emerged as a highly promising technology due to its unique advantages: independence from structural parameters (e.g., mass and stiffness), no reliance on prior information, and capability for three-dimensional deformation reconstruction. The core principle of iFEM involves discretizing the structure into a series of inverse elements, characterizing theoretical strains via nodal displacements, and solving for these displacements by minimizing an error function between theoretical and measured strains, thereby enabling deformation sensing. Nevertheless, in practical aerospace applications, structures often operate under complex loading conditions and boundary constraints. Traditional iFEM approaches face challenges in achieving high-precision deformation reconstruction while maintaining real-time performance, limiting their applicability in mission-critical scenarios. To address these limitations, this study introduces a fundamental optimization of the iFEM framework, which significantly improves the accuracy and real-time performance of deformation sensing of composite antenna panels. Simulation and experimental results show that the proposed iFEM method can further improve the deformation reconstruction accuracy while ensuring real-time performance, and provide a reliable technical support for structural health monitoring under complex working conditions.

Keywords: iFEM, deformation sensing, composite antenna panel, Meshing Strategy, error function¹

Wenpeng Duan, Shenfang Yuan* and Jian Chen, 29 Yudao Street, Research Centre of Structural Health Monitoring and Prognosis, State Key Lab of Mechanics and Control of Aerospace Structures, Nanjing University of Aeronautics and Astronautics, Nanjing 210016, P.R. China

1 INTRODUCTION

Large deployable space phased array antennas are widely used due to their lightweight design, high spatial resolution, and compact packaging [1]. These antennas feature multilayer-heterogeneity composite panels supporting numerous radiofrequency elements with kilowatt-level power consumption[2]. In orbit, these panels experience complex non-uniform thermal loads from solar radiation, cryogenic environments, and internal heat sources, leading to thermal-mechanical deformation that degrades electromagnetic performance [3]. Accurate deformation sensing is therefore critical for real-time radiofrequency compensation and shape control.

Strain-based deformation reconstruction using distributed sensors like Fiber Bragg Gratings (FBG) has gained prominence in aerospace [4]. The inverse finite element method (iFEM) stands out for its full-field reconstruction capability and independence from loading/material properties. iFEM discretizes structures into elements, establishes strain-displacement relationships via deformation theory, and minimizes errors between measured and theoretical strains to determine nodal displacements [5]. Its accuracy depends on element partitioning strategies and error function formulation. Tessler et al. [6] pioneered iFEM in 2003 using 21 triangular elements on a cantilever plate under concentrated load. Cerracchio later adapted it for composite sandwich plates using refined Zigzag theory, testing simply supported and cantilever plates under uniform pressure [7]. Kefal et al. [13, 14] introduced quadrilateral elements to address triangular elements' limited degrees of freedom. These early studies employed uniform element partitioning and single-point strain measurements at element centers.

Recent applications extend iFEM to engineering structures: Niu et al. [8] compared triangular/quadrilateral elements on a small antenna panel, while Poloni et al. [9] analyzed rectangular plates under stretching/bending loads. Abdollahzadeh et al. [10] reconstructed large deformations in clamped laminates using 108 uniform elements, and Li et al. [11] applied iFEM to cryogenic composite tanks. However, these studies focused on simple boundary conditions and mechanical loads, neglecting complex thermal-structural interactions in large multilayer composites [12]. Traditional iFEM struggles with non-uniform thermal loads causing strain gradients and localized concentrations in multilayer antenna panels. Equal-sized elements with center-point strain sampling fail to capture irregular strain distributions, reducing reconstruction accuracy. This highlights the need for optimized element partitioning.

This study proposes a local boundary adaption-based inverse element partition. The partitioning strategy considers internal boundaries, strain concentrations, and thermal gradients to generate adaptive meshes. And experimental verification on an antenna panel prototype.

2 METHOD

2.1 Local boundary adaption-based inverse element partition

The local boundary adaption-based element partition strategy proposed in this paper is implemented in the following steps, as shown in Fig. 1.

(1) In iFEM-based deformation reconstruction, structural boundary conditions are defined by constraining nodal displacements at boundaries. Increased nodal density along boundaries enhances representation accuracy through improved

displacement constraint resolution.

(2) Strain concentration manifests as abrupt strain magnitude transitions within localized regions. To mitigate reconstruction errors, such strain discontinuity zones are confined within dedicated “strain-concentration elements” through targeted mesh refinement, effectively isolating their influence on adjacent regions.

(3) Non-uniform thermal loads induce significant local strain gradients. Two complementary requirements govern element sizing: (a) Element dimensions must remain smaller than characteristic thermal gradient lengths to prevent strain averaging artifacts; (b) Computational efficiency mandates minimal element count while satisfying the first constraint. Our findings indicate a dual-element partitioning across thermal gradient directions achieves optimal balance between accuracy and computational economy, forming “thermal-gradient elements”.

(4) The final adaptive mesh emerges through superposition of three specialized element types: boundary-constrained elements, strain-concentration elements, and thermal-gradient elements.

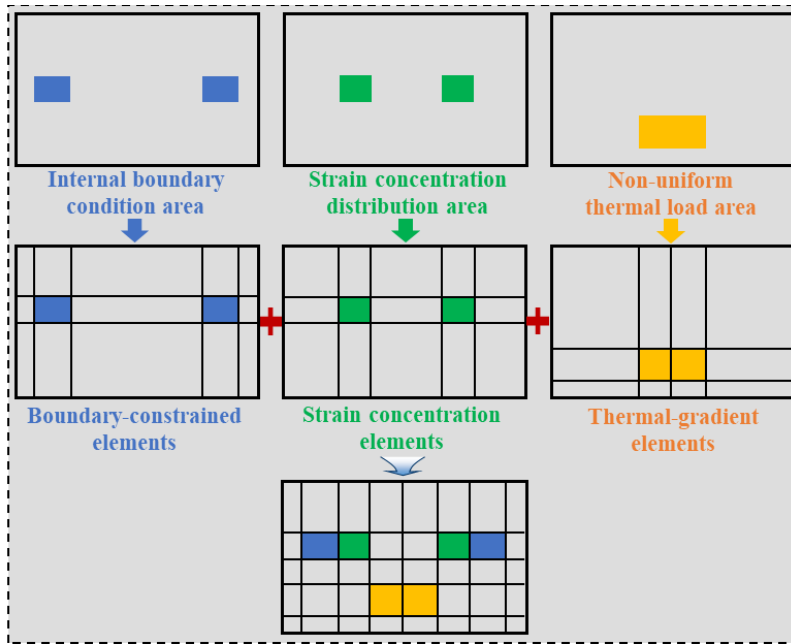


Figure 1 Local boundary adaption-based inverse element partition

2.2 Basics of the iFEM

The error function Φ is defined as Eq. (2). This error function denotes the weighted sum of the squared error between theoretical strain and measured strain at the element center.

$$\Phi(\mathbf{a}^e) = \|\mathbf{e}(\mathbf{a}^e) - \mathbf{e}^\varepsilon\|^2 + (2h)^2 \|\mathbf{k}(\mathbf{a}^e) - \mathbf{k}^\varepsilon\|^2 + \lambda_g \|\mathbf{g}(\mathbf{a}^e) - \mathbf{g}^\varepsilon\|^2 \quad (1)$$

where λ_g is the weight of the transverse shear strain \mathbf{g}^ε , \mathbf{a}^e is the vector of nodal displacements; $\mathbf{e}(\mathbf{a}^e)$ is the membrane strain; $\mathbf{k}(\mathbf{a}^e)$ expresses bending curvature; $\mathbf{g}(\mathbf{a}^e)$ is the transverse shear strain. This input strain is substituted into Eq. (2) to obtain matrices \mathbf{k}^e and \mathbf{f}^e . The \mathbf{K} and \mathbf{F} are obtained by coordinate transformation and element assembly based on the following equations :

$$\mathbf{K} = \sum_{e=1}^{nel} (\mathbf{T}^e)^T \mathbf{k}^e \mathbf{T}^e \quad (2)$$

$$\mathbf{F} = \sum_{e=1}^{nel} (\mathbf{T}^e)^T \mathbf{f}^e$$

where \mathbf{T}^e is coordinate transformation matrix, \mathbf{K} is global coefficient matrix, \mathbf{F} is global coefficient vector.

After that, the problem-specific displacement boundary conditions will be substituted by modifying elements in \mathbf{K} and \mathbf{F} resulting in matrices \mathbf{K}^R and \mathbf{F}^R [6]. Finally, the reconstructed nodal displacements are solved as follows,

$$\mathbf{U}^R = (\mathbf{K}^R)^{-1} \mathbf{F}^R \quad (3)$$

where \mathbf{U}^R is the reconstructed displacement that representing the deformation.

3 EXPERIMENT AND VALIDATION

3.1 Experimental Setup

As shown in Fig. 2, the antenna panel is a multilayer-heterogeneous composite structure, which consists of 0.4 mm (upper skin) / 19.2 mm (aramid paper honeycomb) / 0.4 mm (lower skin). The panel size is 3125mm × 1500mm. The upper and lower skins are made of glass fiber-reinforced epoxy with 4 layers [0°/45°/-45°/90°]. Four T-shaped aluminum blocks that provide the fixed support are embedded to assemble the panel on the antenna truss.

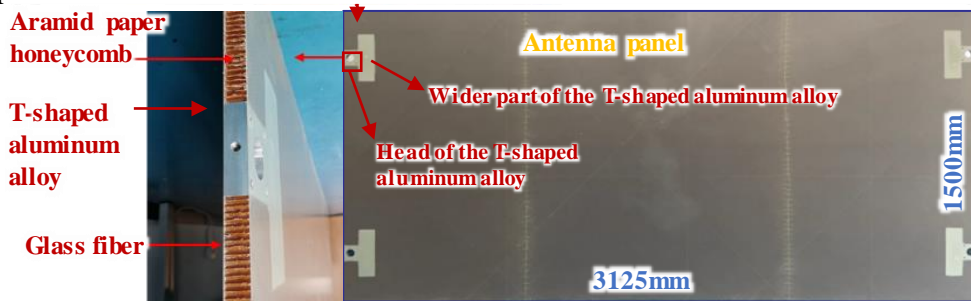


Figure 2 Structural information of the real large deployable satellite antenna panel

The thermal deformation test for the antenna panel is established as shown in Fig. 3. The heads of the T-shaped aluminum blocks are constrained by bolts to provide the fixed boundary condition. The non-uniform thermal load is achieved with a total of 30 polyimide heating films. The high-power supply power provides current for the heating films, such as heating one surface of the antenna panel, which is called the “hot surface”. Conversely, another surface is called the “cold surface”. In addition, laser displacement sensors are used to measure the out-of-plane displacement of the structure. The data acquisition system DH5922D is used to collect displacement data from laser displacement sensors, with a sampling rate of 100Hz.

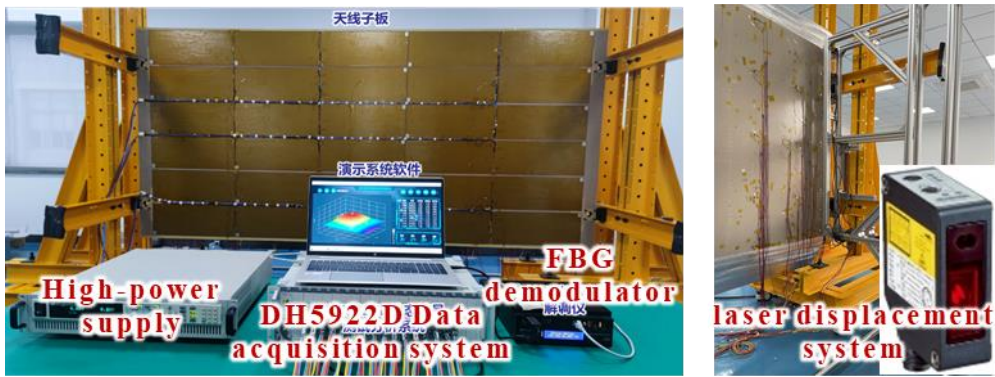


Figure 3 Thermal deformation sensing system of the real antenna panel

3.2 Typical result of deformation reconstruction

The reconstructed displacements and measured displacements at one thermal deformation is shown in Fig. 5. The thermal deformation becomes larger with the heating until the heat balance after 10 minutes. The reconstructed displacement is close to the experimental one. The displacements at different positions are measured by moving the set of laser sensors transversely since the deformation is nearly stable.

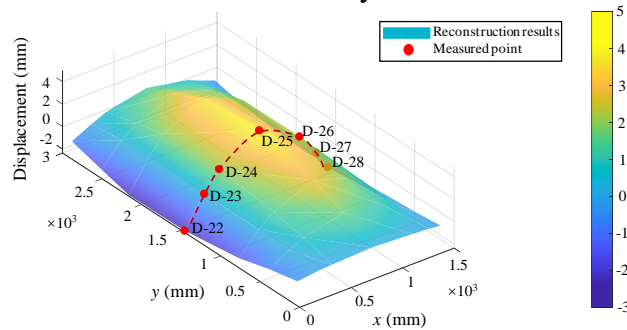


Figure 5 Typical reconstruction results under Experiment-Case 1

3.3 Validation for the LBA-iFEM

3.3.1 Inverse element partition of LBA-iFEM

The antenna panel has the following characteristics: (1) The Mindlin plate theory based on iQS4 applies to thin plates, whose ratio of the thickness to the minimum in-plane size is from 0.01 to 0.2. In this work, the ratio of the antenna panel is 0.13, which means the antenna panel belongs to the thin plate; (2) The antenna panel is a honeycomb core layer structure, which can be simplified into a symmetrical laminated composite thin plate. It is verified that iQS4 is still suitable for the symmetrical laminated composite thin plate by existing studies.

Firstly, the LBA-based element partition is obtained with the follow considerations. The internal boundary conditions are the heads of the T-shaped aluminum blocks. The heads of the T-shaped aluminum blocks are the fixed boundary condition. The wider part of the T-shaped aluminum blocks are divided into elements as strain concentration areas, instead of boundary conditions in the element partition. The dimension of one non-uniform thermal load area is about 625mm×250mm. This paper partitioned these areas into two inverse elements. This element partition is

marked as “Meshing I”. In total, 168 inverse elements are obtained of “Meshing I”. As shown in Figure 4. And to verify the effectiveness of the proposed method, another inverse element partition strategies are used for comparison, as follows: Based on the idea of equal-sized inverse elements partition, the antenna panel is divided into 240 rectangular inverse elements, recorded as “Meshing II”.

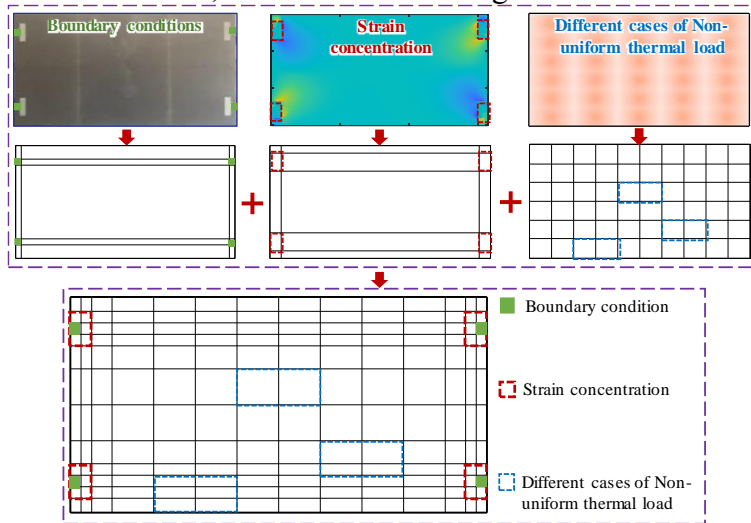


Figure 1 Local boundary adaption-based inverse element partition

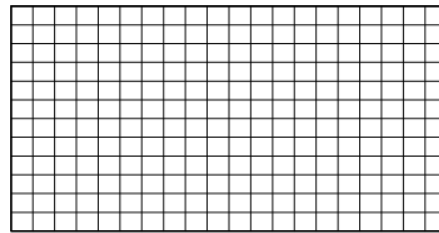


Figure 5 Equal-sized inverse elements partition-based inverse element partition

3.3.2 Deformation reconstruction result

The reconstructed deformation in the middle section is illustrated in Fig. 6. The experimental reconstruction results under the Meshing I and Meshing II are consistent with the experiment reconstruction results. The reconstruction effect of Meshing I more ideal, which is just based on LBA-based inverse element partition. In addition, the reconstruction errors of D22 to D28 at 10 minutes in 5 different experiment non-uniform thermal load are summarized in Figure 6 which shows the E-Max of these methods. In the five experiments, the E-Max of Meshing I is below 0.61mm, which indicates that the error has decreased 49%.

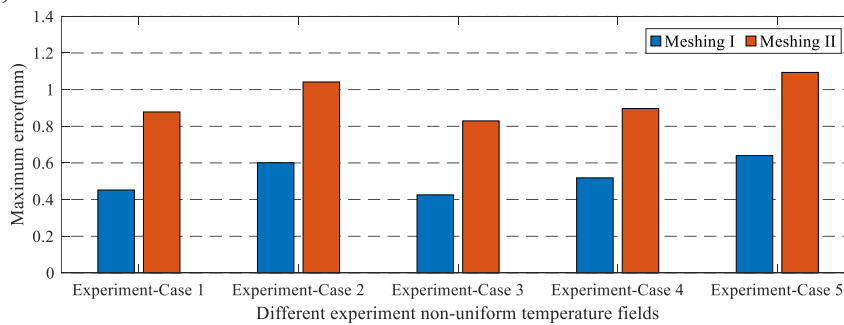


Figure 2 Maximum error of antenna panel under different non-uniform thermal load

4 CONCLUSION

Aiming at the requirements of accurate and robust deformation sensing for large antenna panels, the regional integral iFEM and improved element partition method are proposed. The LBA-based element partition strategy is proposed to discretize the structure into appropriate inverse elements to improve the deformation sensing accuracy and robustness without affecting real-time performance.

In the experimental research, 5 thermal deformation experiments of the antenna panel under different 5 non-uniform thermal loads were carried out. The maximum reconstruction error under all of the experiment non-uniform thermal loads is below 0.61mm. Compared with traditional iFEM, the reconstruction effect of the regional integral iFEM and service element partition method can maximize reconstruction accuracy. In summary, this method effectively improves the reconstruction accuracy and robustness of iFEM under complex and variable working conditions of large structures.

REFERENCES

-
- [1] Pitz, W. The Terra SAR-X Satellite. *IEEE Transactions on Geoscience and Remote Sensing* 2010; 48: 615-622.
 - [2] Lu GY, Zhou JY, Cai GP, et al. Studies of thermal deformation and shape control of a space planar phased array antenna. *Aerospace Science and Technology* 2019; 93: 105311.
 - [3] Du J, Song Y, Bao H. Shape adjustment of cable mesh antennas using sequential quadratic programming. *Aerospace Science and Technology* 2013; 30: 26-32.
 - [4] Xu C. Condition monitoring of composite structure with Fibre Optic Sensors. PhD thesis, Department of Aeronautics, Faculty of Engineering, Imperial College London 2022.
 - [5] Gherlone M, Cerracchio P, Mattone M. Shape sensing methods: Review and experimental comparison on a wing-shaped plate. *Progress in Aerospace Sciences* 2018; 99: 14-26.
 - [6] Tessler A. A variational principle for reconstruction of elastic deformations in shear deformable plates and shells. National Aeronautics and Space Administration, Langley Research Center 2003.
 - [7] Cerracchio P, Gherlone M, Di Sciuva M, et al. A novel approach for displacement and stress monitoring of sandwich structures based on the inverse Finite Element Method. *Composite Structures* 2015 127: 69-76.
 - [8] Niu S, Guo Y, Bao H, et al. A Unified Measurement Method for Shape Sensing of Plate Structure. *IEEE Transactions on Instrumentation and Measurement* 2022; 72: 1-13.
 - [9] Poloni D, Oboe D, Sbarufatti C, et al. Towards a stochastic inverse finite element method: a Gaussian process strain extrapolation. *Mechanical Systems and Signal Processing* 2023; 189: 110056.
 - [10] Abdollahzadeh MA, Ali HQ, Yildiz M, et al. Experimental and numerical investigation on large deformation reconstruction of thin laminated composite structures using inverse finite element method. *Thin-walled structures* 2022; 178: 109485.
 - [11] Li T, Liu M, Li J, et al. Full-field deformation reconstruction for large scale cryogenic composite tanks with limited strain monitoring data. *Smart Materials and Structures* 2023; 32: 115021.
 - [12] Esposito M, Gherlone M. Material and strain sensing uncertainties quantification for the shape sensing of a composite wing box. *Mechanical Systems and Signal Processing* 2021; 160: 107875.